Closely Packed Zeolite Nanocrystals Obtained via Transformation of Porous Amorphous Silica

S. Mintova,*,† M. Hölzl,† V. Valtchev,‡ B. Mihailova,† Y. Bouizi,‡ and T. Bein†

Department of Chemistry, University of Munich (LMU), Butenandtstrasse 11, 81377 Munich, Germany, and UMR-7016 CNRS, ENSCMu, UHA, 3, rue Alfred Werner, 68093 Mulhouse, France

Received December 18, 2003. Revised Manuscript Received July 5, 2004

Amorphous silica grains were subjected to a hydrothermal treatment to be transformed into closely packed ZSM-5 zeolite nanocrystalline bodies. Three synthesis approaches have been developed: (I) direct hydrothermal treatment of the amorphous silica grains in a ZSM-5 precursor solution; (II) impregnation of charge-reversed amorphous silica grains with 2−10 nm preorganized units followed by a hydrothermal treatment in a silica-free precursor synthesis solution; and (III) electrostatic adsorption of 50-nm sized ZSM-5 seeds on the amorphous silica grains followed by a hydrothermal treatment with a ZSM-5 precursor solution. The synthesized solids were characterized by X-ray diffraction, Raman spectroscopy, TG analysis, N_2 adsorption measurements, and scanning electron microscopy. The resulted zeolitic bodies are built of uniform closely packed nanocrystals and retain the size and morphological features of the initial amorphous silica grains. The crystallinity, the average size of crystallites, and the mechanical properties of the nanozeolite bodies depend strongly on the synthesis procedure. It was found that procedure II provides mechanically stable bodies built of closely packed nanocrystallites with a size of about 40 nm, which are very promising for the production of self-bonded nanozeolite structures.

Introduction

Synthetic zeolites and related molecular sieves are generally produced as powders of relatively loosely bonded zeolite particles with sizes ranging from 500 nm to several micrometers. The main applications of these materials are in the area of heterogeneous catalysis, ion exchange, and gas separations where the zeolite powders are used in the form of agglomerates with desired shape and size.[1] Optimal utilization of zeolites requires that they can be formed to or incorporated in bodies with shapes and properties adapted to the process requirements. Depending on the actual application, factors such as mechanical strength, attrition resistance, shape and size of bodies, and porosity (pore size, pore size distribution, etc.) have to be optimized to prolong the lifetime of the material and to avoid an extensive pressure drop over the reactor in which the material is charged, or to minimize the effects of diffusion. Agglomerates of molecular sieves used in practical applications are commonly prepared by adding an inorganic binder (clays, silica, alumina) to the molecular sieve powder to produce a wet mixture. This mixture is then extruded into cylindrical pellets, formed into beads by granulation, or spray-dried into small spherical particles, whereafter the material is dried and calcined to convert the clay into an amorphous binder providing the material with a high mechanical strength. In such bodies, the fact that the zeolite is diluted with a material that in most instances is inert in the process reduces the effective surface area of the product. Moreover, the utilization of the molecular sieve is often limited by diffusion limitations imposed by the binder system used.

During the past decade, the syntheses and the applications of zeolite nanocrystals have gained considerable attention. The most interesting zeolite materials from an industrial point of view, that is, FAU-,[2] LTA-,[2] MFI-,[3] LTL-,[4] BEA-type[5] structures, have been prepared in the form of stable colloidal suspensions of monodisperse nanocrystals. Nanozeolites are expected to have a great impact on the performance of zeolite catalysts because of the reduced transport paths via zeolite micropores and a substantial increase of the external surface area.[6−9] However, negative effects, such as blocking of the micropores by the inorganic binder, will be more pronounced if nanoparticles are used for preparation of the conventional molecular sieve ag-

* Corresponding author. Fax: +4989 2180 77622. E-mail: svetlana.mintova@cup.uni-muenchen.de.
† University of Munich (LMU).
‡ UMR-7016 CNRS.

(1) Breck, D. W. *Zeolite Molecular Sieves: Structure, Chemistry and Use*; Wiley & Sons: New York, 1972.
(2) Schoeman, B. J.; Sterte, J.; Otterstedt, J.-E. *Zeolites* **1994**, *14*, 110.
(3) Persson, A. E.; Schoeman, B. J.; Sterte, J.; Otterstedt, J.-E. *Zeolites* **1994**, *14*, 557.
(4) Tsapatsis, M; Lovallo, M.; Okubo, T.; Davis, M. E. *Mater. Res. Soc. Symp. Proc.* **1995**, *371*, 21.
(5) Camblor, M. A.; Corma, A.; Misud, A.; Perez-Pariente, J.; Valencia, S. *Stud. Surf. Sci. Catal.* **1996**, *105A*, 341.
(6) Rajagopalan, K.; Peters, A. W.; Edwards, G. C. *Appl. Catal., A* **1986**, *23*, 69.
(7) Camblor, M. A.; Corma, A.; Valencia, S. *Microporous Mesoporous Mater.* **1998**, *25*, 59.
(8) Landau, M. V.; Tavor, D.; Regev, O.; Kaliya, M. L.; Hreskowitz, M.; Valtchev, V.; Mintova, S. *Chem. Mater.* **1999**, *11*, 2030.
(9) Landau, M. V.; Vradman, L.; Valtchev, V.; Lézervant, J.; Liubich, E.; Talianker, M. *Ind. Eng. Chem. Rev.* **2003**, *42*, 2773.

10.1021/cm030640b CCC: $27.50
Published on Web 11/11/2004

glomerates by conventional methods. Hence, methods that allow the preparation of binderless bodies built of zeolite nanocrystals are highly desired.

Pressure forming of a zeolite powder can be used for the preparation of binderless bodies. However, such bodies suffer of a limited mechanical strength and uncontrolled porosity. Other approaches for the preparation of binderless zeolite bodies are the direct hydrothermal transformation of volcanic glasses[10] and densified aluminosilicate gels[11] into self-bonded zeolite pellets. In these materials, the effect of dilution with an inert inorganic binder is obviously avoided. However, such materials are not fully utilizable in some processes because of diffusion limitations due to the large size of the zeolite crystals and the high density of the bodies. Mesoporous silica pellets have been used for the synthesis of ZSM-5 nanocrystals.[12,13] Indeed, small zeolite particles (25 nm) were formed in the mesopores, but much larger crystals (>500 nm) were found in the macropores and external surface of the pellets. More uniform micro/macroporous zeolite bodies have been prepared by Stein and co-workers using a dual templating approach.[14] Similar bodies were prepared by self-assembling of monodisperse zeolite nanocrystals and polystyrene spheres and a subsequent hydrothermal synthesis procedure.[15] The calcination of the composite provides organized micro/macropore structures. The use of preformed zeolite nanoparticles and specific macrotemplates allowed the synthesis of zeolite structures with controlled macromorphology and very often with hierarchical organization. For example, ordered macroporous zeolite fibers have been prepared by infiltration of zeolite nanocrystals into bacterial threads.[16] Wood cell[17] and starch gel[18] templating provided microporous zeolite monoliths. A large variety of synthetic[19−23] and biological[24−26] templates have been employed to obtain controlled assemblies of zeolite nanoparticles. These synthesis approaches, however, require a relatively complicated preparation procedure and often expensive macrotemplates.

The present study describes a facile and efficient way for synthesis of self-bonded bodies built of closely packed zeolite nanoparticles via structural transformation of micrometer-sized porous amorphous silica grains.

Experimental Section

Materials. Ultrapure porous amorphous silica grains (99.99% SiO_2) with a size of 60 μm and an average pore diameter of 5 nm (Acros Organics) were used for the synthesis of nanozeolite bodies. A cationic polymer (Redifloc 4150, Akzo Nobel, Sweden) was applied as a charge-reversing agent. A colloidal ZSM-5 suspension prepared according to the conditions given below was used for seeding of the pure amorphous silica grains.

Preparation of ZSM-5 Colloidal Suspension. The synthesis solutions used for the preparation of sols of ZSM-5 nanocrystals (MFI-type structure) and for the transformation of the amorphous silica grains according to procedures I and III (see the section below) had the following chemical composition: $9TPAOH:0.25Al_2O_3:25SiO_2:599H_2O$. The initial solutions were prepared by mixing tetraethyl orthosilicate (TEOS, 98%, Aldrich), aluminum isopropoxide (AlIso, 99.99%, Aldrich), and tetrapropylammonium hydroxide (TPAOH, 1 M aqueous solution, Aldrich). The silica and alumina alkoxydes were hydrolyzed under slow stirring (50 rpm) for 24 h at room temperature. The alcohols issued from the silica and alumina sources were evaporated for 5 h at 40 °C under stirring. The water weight loss due to the evaporation process was compensated by adding distilled water in the initial solution. The obtained clear solutions were transferred in polypropylene (PP) bottles and subjected to hydrothermal (HT) treatment in a conventional oven. The syntheses were performed at 90 °C for 18 h. After the treatment, the zeolite suspensions were purified in a series of four steps consisting of high-speed centrifugation (20 000 rpm, 1 h), removal of the mother liquor, and redispersion in doubly distilled water. The pH of the purified ZSM-5 zeolite suspensions was adjusted to about 9.5 by the addition of a 0.10 M NH_3 solution. The mass content of the zeolite crystals in the aqueous suspensions was about 3 wt %.

Transformation of the Amorphous Porous Silica Grains into Closely Packed Nanozeolite Bodies. The transformation process from amorphous porous silica grains into closely packed zeolite bodies was carried out using three different procedures.

Procedure I: 5.0 g of amorphous silica grains was subjected to direct HT treatment with 40 g of initial precursor solutions at 90 °C for 18 h.

Procedure II: To keep the overall composition of the system constant, 8.35 g of amorphous porous silica grains was soaked in 40 g of cationic polymer (Redifloc 0.5 wt %) for 1 h under ultrasonic radiation. After the charge-reversal step, the amorphous silica grains were soaked in 100 g of 1-week aged ZSM-5 precursor solution. This procedure was repeated three times. Finally, the HT synthesis was performed with 35.75 g of precursor solution having the same composition as that used in procedure I but without silica (denoted as silica-free initial solution) at 90 °C for 18 h.

Procedure III: (i) 5.0 g of amorphous porous silica grains was soaked in 40 g of cationic polymer (Redifloc 0.5 wt %) for 1 h under ultrasonic radiation; (ii) 50 nm ZSM-5 crystals redispersed in water (solid content ≈ 1.8 wt %) were electrostatically adsorbed on charge-reversed amorphous silica grains under an ultrasonic treatment at ambient temperature for 30 min; and (iii) the pretreated silica grains were hydrothermally treated with 40 g of ZSM-5 precursor solution at 90 °C for 18 h. Note: after stages (i) and (ii), the amorphous silica grains were separated from the solution and rinsed with a 0.1 M NH_3 solution and distilled water.

After the syntheses, the zeolite bodies were separated from the zeolite nanocrystals formed in the bulk solutions, washed, and dried. Half of each sample was calcined in airflow at 550 °C for 5 h.

Characterization of the Closely Packed Nanozeolite Bodies. The particle size analysis of the amorphous and

(10) Aiello, R.; Nastro, A.; Colella, C. *Zeolites* **1982**, *2*, 290.
(11) Crea, F.; Aiello, R.; Natrso, A.; Nagy, J. B. *Zeolites* **1991**, *11*, 521.
(12) Landau, M. V.; Zaharur, N.; Hreskowitz, M. *Appl. Catal., A* **1994**, *115*, 7.
(13) Landau, M. V.; Hreskowitz, M. *Stud. Surf. Sci. Catal.* **1995**, *94*, 357.
(14) Holland, B. T.; Abrams, L.; Stein, A. *J. Am. Chem. Soc.* **1999**, *121*, 4308.
(15) Valtchev, V. *J. Mater. Chem.* **2002**, *12*, 1914.
(16) Zhang, B.; Davis, S. A.; Mendelson, N. H.; Mann, S. *Chem. Commun.* **2000**, 781.
(17) Dong, A.; Wang, Y.; Tang, Y.; Ren, N.; Zhang, Y.; Yue, Y.; Gao, Z. *Adv. Mater.* **2002**, *14*, 926.
(18) Zhang, B.; Davis, S. A.; Mann, S. *Chem. Mater.* **2002**, *14*, 1369.
(19) Rhodesn, K. H.; Davis, S. A.; Caruso, F.; Mendelson, N. H.; Zhang, B.; Mann, S. *Chem. Mater.* **2000**, *12*, 2832.
(20) Tosheva, L.; Valtchev, V.; Sterte, J. *Microporous Mesoporous Mater.* **2000**, *35−36*, 621.
(21) Lee, Y.; Lee, J. S.; Park, Y. S.; Yoon, K. B. *Adv. Mater.* **2001**, *13*, 1259.
(22) Valtchev, V.; Schoeman, B. J.; Hedlund, J.; Mintova, S.; Sterte, J. *Zeolites* **1996**, *17*, 408.
(23) Huang, I.; Wang, Z.; Sun, J.; Liao, I.; Li, Q.; Yan, Y.; Zhao, D. *J. Am. Chem. Soc.* **2000**, *122*, 3530.
(24) Anderson, M. W.; Holms, S. M.; Hanif, N.; Cundy, C. S. *Angew. Chem., Int. Ed.* **2000**, *39*, 2707.
(25) Wang, Y.; Tang, Y.; Dong, A.; Wang, X.; Ren, N.; Gao, Z. *J. Mater. Chem.* **2002**, *12*, 1812.
(26) Valtchev, V.; Smaihi, M.; Faust, A.-C.; Vidal, L. *Angew. Chem., Int. Ed.* **2003**, *42*, 2782.

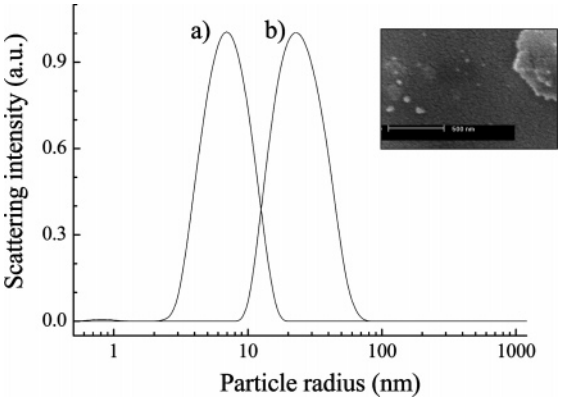

Figure 1. DLS data of (a) ZSM-5 precursor solution aged at room temperature for 1 week and (b) ZSM-5 suspension after hydrothermal treatment at 90 °C for 18 h. The DFA is displayed as scattering intensity per unweighted particle size classes. Inset: SEM micrograph of the ZSM-5 nanocrystals used for seeding of the amorphous silica grains.

crystalline entities in the precursor solutions and ZSM-5 crystalline suspensions was performed with an ALV-NIBS/HPPS particle size analyzer operating at a scattering angle of 173° with an incident laser wavelength of 632.8 nm and an output power of 3 mW. The powder X-ray diffraction (XRD) data were collected on a STOE STADI-P diffractometer in Debye−Scherer geometry equipped with a linear position-sensitive detector and employing Ge-monochromated Cu Kα radiation. The Raman spectra of as-prepared and calcined samples were measured with a Bruker Equinox 55 FT-IR spectrometer equipped with a FRA106/S FT-Raman module and a liquid N_2 cooled Ge detector, using the 1064 nm line of an Nd:YAG laser with an output laser power of 500 mW. Micrographs of the amorphous silica grains and nanozeolite bodies were taken with a Philips XL 40 scanning electron microscope (SEM). The combined TG/DSC analyses of the samples were performed with a Setaram TG-ATD LABSYS thermal analyzer with a heating rate of 5 °C min^{-1} in an atmosphere containing 80% N_2 and 20% O_2. Nitrogen adsorption/desorption measurements were carried out on calcined samples with a Micromeritics ASAP 2010 surface area analyzer. Prior to analysis, the samples were outgassed overnight at 350 °C. Surface areas were calculated using the BET equation, pore size distributions were determined by the BJH method, and micropore volume was obtained via *t*-plot analysis. The chemical composition of the samples was determined by inductively coupled plasma atomic emission spectrometry, ICP-AES (Varian).

Results

ZSM-5 Nanocrystals Used for Seeding the Amorphous Silica Grains. The distribution function analysis (DFA) data of the colloidal particles before and after hydrothermal treatment are depicted in Figure 1. The presence of colloidal particles with sizes ranging between 2 and 10 nm was measured in the ZSM-5 precursor solution after 1 week of aging at ambient conditions (Figure 1a). The DLS data show that these small species are stable and further aging does not change their size. Powder XRD study of these particles did not reveal any crystallinity. After 18 h of hydrothermal treatment, particles with a mean radius of about 25 nm were observed by DLS (Figure 1b). These particles have a monomodal particle size distribution and form a very stable colloidal suspension in water. The solid product extracted from this suspension is entirely crystalline and has an XRD pattern identical

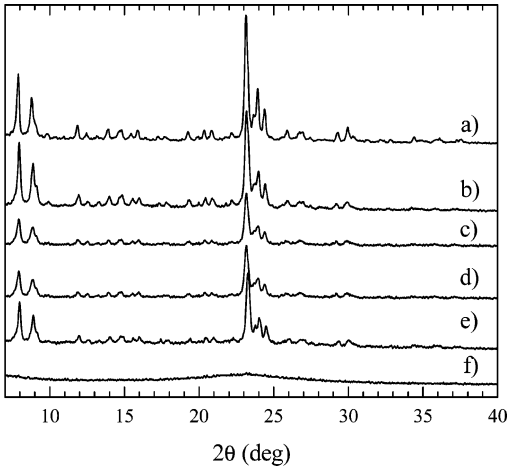

Figure 2. XRD patterns of (a) highly crystalline ZSM-5 zeolite, (b) ZSM-5 nanocrystals used for seeding, and closely packed zeolite bodies obtained via (c) procedure III, (d) procedure II, (e) procedure I, and (f) untreated porous amorphous silica grains.

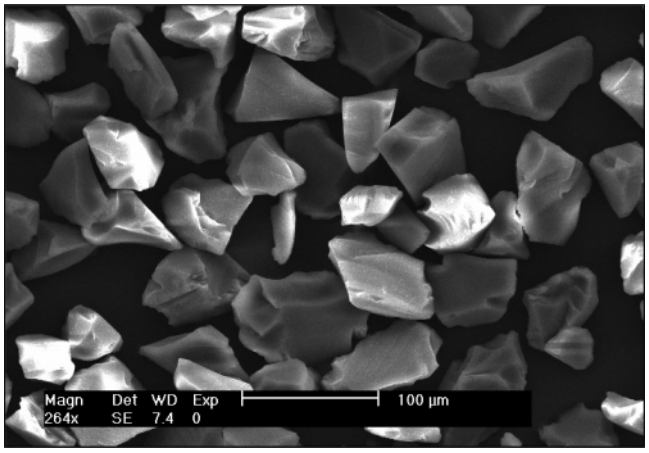

Figure 3. SEM micrograph of untreated amorphous silica grains.

to that of a highly crystalline ZSM-5 type zeolite with MFI structure (see Figure 2a,b). As can be seen in the inset of Figure 1, the solid product consists of uniform in size particles with spheroidal shape and morphology typical for colloidal zeolite nanocrystals. The prolongation of the synthesis time up to 20 h resulted in the formation of ZSM-5 nanocrystallites with a mean radius of about 30 nm; no substantial increase in the particle size was observed under further prolonging the hydrothermal treatment.

Nanozeolite Bodies Prepared According to Procedure I. The initial amorphous silica grains before any manipulation are shown in Figure 3. The initial silica grains were mixed with the precursor synthesis solution and subjected to direct HT treatment. This procedure does not include preliminary seeding of the amorphous silica grains. The XRD pattern of the material (Figure 2e) showed crystallinity similar to that of the ZSM-5 nanocrystrals prepared for seeding (Figure 2b). The SEM inspection shows that the morphological features of the initial silica grains are retained (Figure 4a). However, the ZSM-5 crystals (about 200 nm) building the nanozeolite bodies are not closely packed, and cracks with lengths of up to several micrometers can be seen on the grain surfaces (Figure 4b).

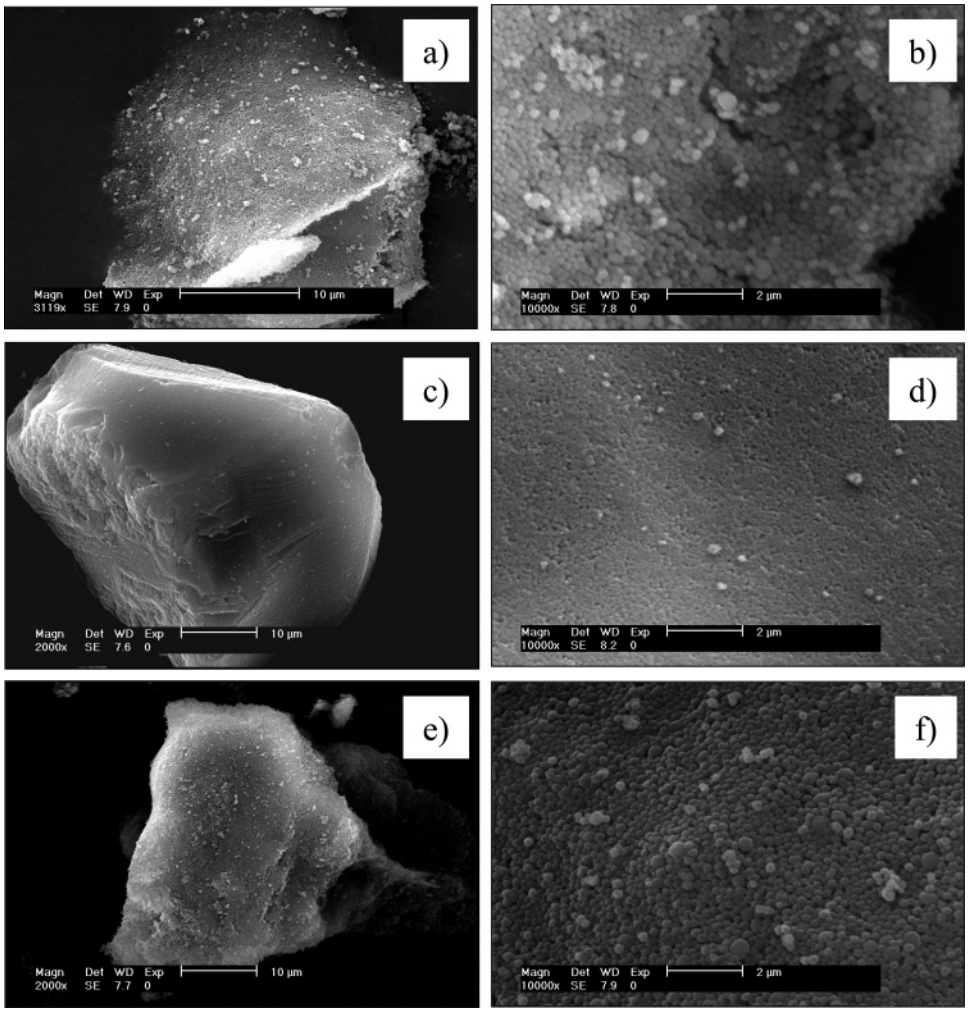

Figure 4. SEM micrographs of as-prepared closely packed nanozeolite bodies prepared via procedure I at different magnifications (a) $M = 10$ μm and (b) $M = 2$ μm, via procedure II at different magnifications (c) $M = 10$ μm and (d) $M = 2$ μm, and according to procedure III at different magnifications (e) $M = 10$ μm and (f) $M = 2$ μm.

Nanozeolite Bodies Prepared According to Procedure II. The second synthesis procedure includes impregnation of the amorphous silica grains with the 2−10 nm entities formed in the ZSM-5 precursor solution. The recent studies on similar initial systems have shown that these primary particles already possess crystalline domains.[27,28] It was expected that some of these preorganized units could penetrate deeply in the bulk of the silica grains and induce crystallization not only on the surface but also into the bulk of the grain. To increase the bulk loading, the amorphous silica grains were soaked three times in a week-aged initial solution. Another specific feature of this synthesis procedure is that the precursor solution used for further HT treatment does not contain any silica.

According to the XRD pattern, the synthesized material has a high crystallinity (Figure 2d), and it retains the size and the macromorphological features of the initial silica grains (Figure 4c). A high-magnification view at the resulted agglomerates shows that they are built of uniform, small particles with a size of about 40 nm (Figure 4d). These nanocrystallites are closely packed, and no gaps between individual nanoparticles can be observed.

The successful transformation of the amorphous silica grains into aggregates of closely packed ZSM-5 nanocrystallites is most probably due to the homogeneous crystallization process inside the presoaked silica grains. Charge-reversed macroporous silica grains adsorbed the 2−10 nm nanoparticles, thus inducing the zeolite crystallization inside of the bulk during the HT treatment. The absence of silica in the synthesis solution probably also contributes to the high degree of close packing of the zeolite nanocrystals in the final self-assembled bodies.

Nanozeolite Bodies Prepared According to Procedure III. The ZSM-5 colloidal crystals (diameter ∼50 nm) obtained after 18 h of HT treatment were used for seeding of amorphous porous silica grains. As known, in basic media, both the amorphous silica and the zeolite nanocrystals are negatively charged, which prevents their interaction. To facilitate the adsorption of zeolite seeds, the surface charge of the amorphous silica was reversed (see Experimental Section). The charge-reversed amorphous silica grains were then transferred in ZSM-5 crystalline colloidal suspension so as to electrostatically adsorb nanocrystals.

(27) Kirschhock, C. E. A.; Buschmann, V.; Kremer, S.; Ravishankar, R.; Houssin, C. J. Y.; Mojet, B. L.; van Santen, R. A.; Grobet, P. J.; Jacobs, P. A.; Martens, J. A. *Angew. Chem., Int. Ed.* **2001**, *40*, 2637.

(28) Mintova, S.; Olson, N. H.; Senker; J.; Bein, T. *Angew. Chem., Int. Ed.* **2002**, *41*, 2558.

According to the XRD data, a highly crystalline MFI-type material was obtained after 18 h of heating (Figure 2c). The overall size and shape of the synthesized nanozeolite bodies are nearly identical to those of the initial amorphous silica grains (Figure 4e); that is, the synthesized material retains the macromorphological features of the silica grains. The calcination of the material at 550 °C did not provoke any changes in the morphology of the resulted bodies. At high magnification, uniform individual spheroidal particles with a size of about 200 nm and certain number of larger crystals at the grain surfaces can be seen in the SEM image (Figure 4f). In general, the nanocrystals are closely packed, but still the individual crystals can be distinguished.

The initial silica grains are mesoporous with an average pore size of about 5 nm, which makes impossible the penetration of the 50 nm ZSM-5 zeolite nanocrystals into the grain bulk. Therefore, the adsorption of zeolite nanocrystals takes place mainly at the external surface of the silica grains and cannot influence the crystallization process in the bulk of the amorphous grains.

The characterization of the obtained bodies of ZSM-5 nanoparticles was completed by TG, N_2 adsorption, and Raman measurements.

Chemical Analysis. The chemical analyses revealed that the Si/Al ratio of the nanozeolite bodies is in the range of 42−47. In particular, the Si/Al ratio of the samples prepared according to procedures I and III was 42.1 and 43.8, respectively. The highest Si/Al ratio, that is, ∼47, showed the nanozeolite bodies prepared according to procedure II. It has to be noticed that in the latter case the entire silica was introduced as SiO_2 porous amorphous grains. Probably this is the reason for almost total hydrothermal conversion of the amorphous silica into ZSM-5 nanozeolite bodies. In procedures I and III, the silica comes from two different sources, that is, silica grains and tetraethyl orthosilicates, which might be the reason for the lower silica conversion with respect to procedure II.

TG Analysis. The TG analysis shows that the weight loss of the amorphous silica grains is 2.5 wt % in the temperature range 25−800 °C (Figure 5a). The total weight loss of ZSM-5 nanocrystals used as seeds is 13.9 wt %, which includes the water loss (2.7 wt %) in the temperature range 25−210 °C and the combustion of the organic structure directing agent (SDA) between 270 and 500 °C (11.2 wt %) (figure is not shown).

The TG analysis of the sample prepared according to procedure I shows a total weight loss of 14.8 wt % (Figure 5b). The weight loss (3.5 wt %) in the temperature range 25−250 °C, coupled with a well-distinguished endothermic effect, was attributed to loosely bound water. The main weight loss of 11.3 wt % is in the temperature range 250−500 °C, where the thermal degradation of the SDA takes place. The sample synthesized according to procedure III showed fairly similar weight losses in the temperature ranges of 25−250 and 250−500 °C. In contrast, the sample obtained by procedure II shows much higher mass loss (7.4 wt %) in the low-temperature range (25−250 °C), and in the high-temperature range the loss is about 10.4 wt % (Figure 5c). The first weight loss was attributed to

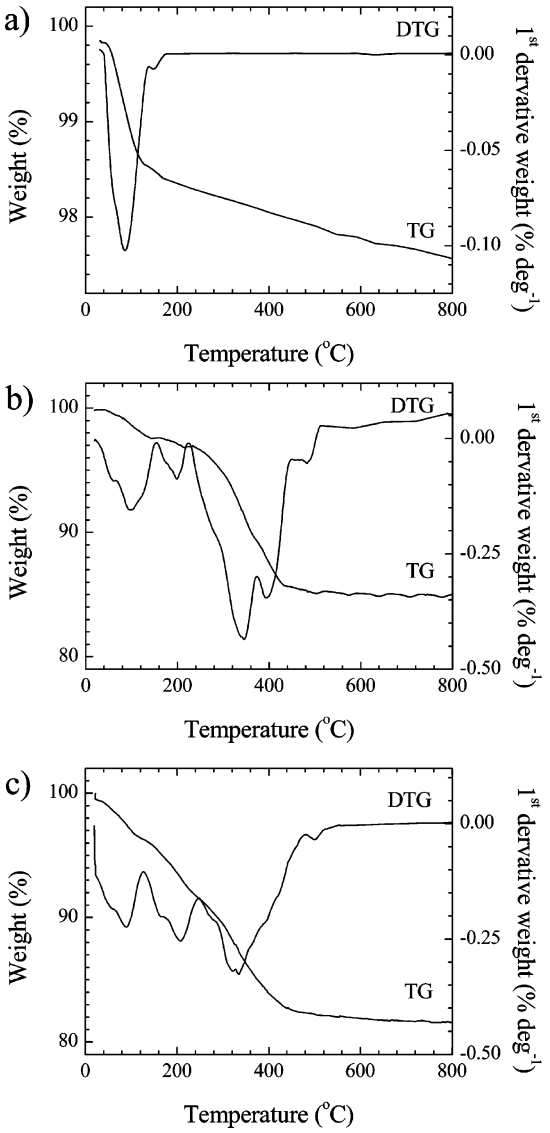

Figure 5. TG/DTG curves of (a) untreated amorphous silica grains, and closely packed nanozeolite bodies prepared according to (b) procedure I, and (c) procedure II.

desorption of loosely bound water and decomposition of SDA adsorbed at the surface of the particles. This relatively high weight loss observed at low temperature suggests the presence of a highly hydrated amorphous material. The combustion of the SDA occluded in zeolite pores is slightly shifted to the low-temperature range with respect to the other two samples. The decomposition at a lower temperature of the occluded SDA is most probably due to the smaller crystals synthesized by procedure II as compared to those obtained via procedures I and III as revealed by SEM (Figure 4).

Nitrogen Sorption Study. The specific surface areas of the amorphous silica grains and calcined nanozeolite bodies obtained according to different synthesis procedures were determined by nitrogen adsorption. The amorphous silica grains possess a specific surface area of 540 $m^2\ g^{-1}$. The adsorption/desorption isotherms shown in Figure 6a indicate the presence of micro- and mesopores in the material; that is, after the steep rise in the gas uptake at low relative pressures that corresponds to the filling of the micropores with N_2, an inclination of the curve with the increase of

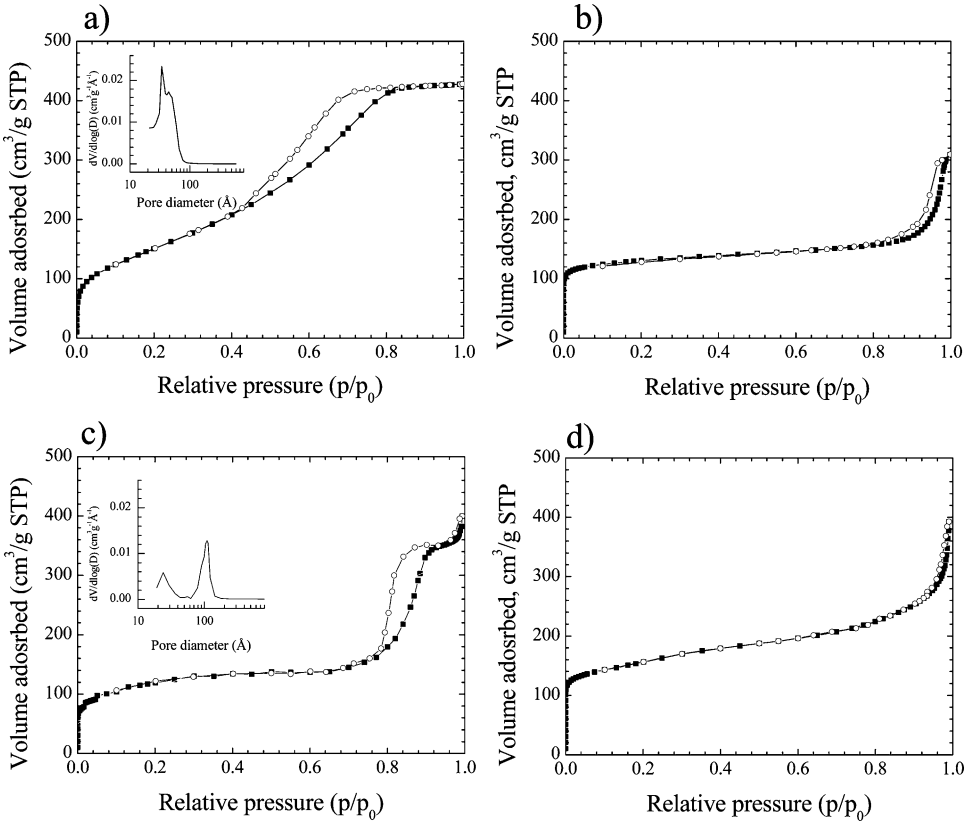

Figure 6. Adsorption/desorption isotherms of (a) untreated amorphous silica grains, and closely packed zeolite bodies synthesized according to (b) procedure I, (c) procedure II, and (d) procedure III.

pressure can be observed. At high relative pressures, the upward turn with a hysteresis loop is indicative of the generation of intergrain mesoporosity. According to the BJH calculation, the major part of these textural pores is in the mesopore range 30−80 Å with a sharp maximum at about 50 Å (Figure 6a, inset). The HT treatment according to procedure I provided a material with completely different characteristics. The micropore volume (0.142 $m^3\ g^{-1}$) due to the zeolite formation is much higher than that of the initial silica grains (0.061 $cm^3\ g^{-1}$). However, the intergrain mesoporosity disappeared, and only traces of relatively large mesopores were detected by the BJH analysis (not shown here). The specific surface area of the material is 471 $m^2\ g^{-1}$, which is somewhat higher than that of a pure MFI-type and most probably due to impurities of high surface area amorphous material present in this sample. Both the specific surface area (480 $m^3\ g^{-1}$) and the micropore volume (0.136 $cm^3\ g^{-1}$) of the sample synthesized according to procedure III are similar to those of the sample prepared via procedure I (Figure 6b,d). In contrast, nanozeolite bodies obtained by procedure II showed a lower micropore volume (0.104 $m^3\ g^{-1}$), which could be interpreted as a lower level of HT transformation of the initial silica grains into MFI-type material, or as blockage of the pore openings for adsorption and debris within the pore structure. On the other hand, the size of the crystals is significantly smaller, which could be the reason for the observed lower pore volume. A similar phenomenon has already been reported for zeolite beta nanocrystals by Camblor et al.[7] The adsorption/desorption isotherms and the BJH pore size analysis clearly identified the presence of distinctive mesopores (Figure 6c). After the steep uptake at low relative pressures that corresponds to the filling of the micropores with N_2, an inclination of the curve with two distinctive hysteresis loops at 0.6−0.85 and 0.96−1.0 relative pressure ranges (P/P_0) are observed. According to the BJH calculation, the major part of these textural mesopores is in the range 20−200 Å with a sharp maximum at about 110 Å (Figure 6c, inset). Thus, the zeolite bodies obtained according to the second synthesis procedure possess combined micro/mesoporosity.

Raman Spectroscopic Study. The local structure of the as-synthesized and calcined closely packed zeolite bodies was additionally studied by Raman spectroscopy. Figure 7 presents the spectra of as-synthesized samples obtained according to procedures I, II, and III as well as the X-ray amorphous sample prepared for 14 h of treatment according to procedure I. The Raman spectra of ZSM-5 bulk sample prepared in the absence of silica grains and of the organic template solution (1 M TPAOH) were also plotted as reference spectra. The Raman scattering of noncalcined zeolite-type materials is dominated from the signals arising from the atomic vibrations of the organic template. The TPA ions occluded in the MFI structure have a specific conformation which differs from that of TPA ions trapped in a disordered network of TO_4 tetrahedra (T = Si,Al).[29] The different conformations of TPA ions can easily be distinguished through the Raman scattering in the range 2800−3100 cm^{-1} originated from the C−H bond stretching as well as through the Raman bands near 1330 and 1140 cm^{-1} related to vibrations of the CH_2 groups. As seen in Figure 7e, the Raman scattering

(29) Li, Q.; Mihailova, B.; Creaser, D.; Sterte, J. *Microporous Mesoporous Mater.* **2001**, *43*, 51.

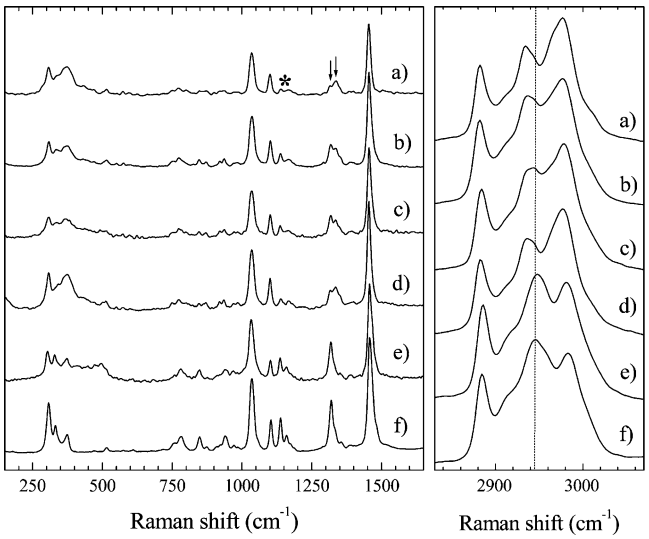

Figure 7. Raman spectra of (a) as-prepared ZSM-5 powder nanocrystals used as a reference sample; as-prepared closely packed nanozeolite bodies via (b) procedure I for 18 h HT treatment, (c) procedure II for 18 h HT treatment, (d) procedure III for 18 h HT treatment, (e) procedure I for 14 h HT treatment, and (f) pure TPAOH; the dashed line traces the position of the C−H stretching peak in the spectrum of TPAOH for which the lower-energy shift due to interactions between TPA and T−O network atoms is most pronounced; the asterisk marks the Raman band near 1140 cm^{-1}, whose relative intensity is suppressed if TPA molecules are embedded in the ZSM-5 zeolite nanocrystals; the arrows point to the Raman peaks at 1315 and 1335 cm^{-1}, whose intensity ratio is most indicative for the presence of TPA incorporated in the MFI structure.

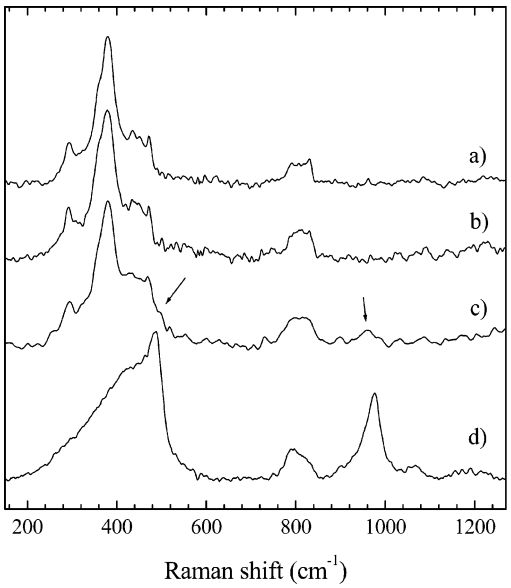

Figure 8. Raman spectra of (a) calcined ZSM-5 zeolite nanocrystals, calcined nanozeolite bodies obtained via (b) procedure I, (c) procedure II, and (d) porous amorphous silica grains. The arrows for curve (c) mark the extra Raman signals due to structural defects in the ZSM-5 crystals self-bonded in nanozeolite bodies.

generated by the atomic vibrations of TPA occluded in the amorphous material obtained for 14 h of treatment according to procedure I resembles that of pure TPAOH. The Raman spectra of all of the three crystalline samples show the features that are characteristic of MFI-type structure: (i) a red shift and a change in the relative intensity of the C−H bond stretching modes, (ii) a frequency splitting of the peak near 1330 cm^{-1}, and (iii) a decrease in the relative intensity of the peak near 1140 cm^{-1}. However, the spectrum of the sample prepared according to procedure I is similar to the reference powder ZSM-5, while for the samples prepared via procedures II and III, some spectral variations related to the TPA modes are observed. The intensity ratio between the Raman signals at 1335 and 1315 cm^{-1} for the latter two samples is less than unity, whereas for entirely crystalline ZSM-5 samples should be higher than unity (Figure 7a). In addition, the Raman scattering near 1140 cm^{-1} is suppressed in a lower degree for samples prepared via procedures II and III in comparison to the reference ZSM-5 powder. These spectral peculiarities indicate that in the samples prepared via procedures II and III exist TPA ions that are not twisted to adapt the porous MFI-type structure. These TPA ions may be adsorbed on the surface of the ZSM-5 crystallites or trapped in relatively large cavities inside non- or poor-crystalline T−O domains. Further, there are slight differences between the spectra of the samples prepared via procedures II and III, suggesting differences in the degree of structural disorder. For the sample prepared according to procedure II, one observes (i) the smaller lower-energy shift of the peak near 2945 cm^{-1}, (ii) smaller intensity ratio between signals at 1335 and 1315 cm^{-1}, and (iii) subtle additional Raman scattering in the range 400−500 cm^{-1}. This might be due to the small crystal size of ZSM-5 particles forming the nanozeolite bodies in sample II. It has been shown that the smaller crystals have more interruptions in the T−O network, leading to the formation of more defects. For instance, about 7% of the silica in a micrometer-sized MFI-type material is present as SiOH,[30] while for the nanosized MFI-type material the amount of silanols exceeds 13%.[31] Because of the overlapping between the peaks generated by the T−O network and by the TPA ions, the structural state of the T−O network can be better estimated by considering the Raman spectra of the calcined samples. Thus, to give more insight on the structural peculiarities of the samples prepared according to procedures I and II, the Raman spectra of the calcined samples were collected (Figure 8). Characteristic spectral features of the porous amorphous silica grains are (i) an intense broad band centered at about 430 cm^{-1} and an intense sharp peak at 490 cm^{-1}, which is typical of disordered three-dimensional Si−O networks, and (ii) an intense peak at 976 cm^{-1}, resulting form the large amount of broken Si−O−Si linkages due to the porosity of the Si−O network. The Raman spectrum of the zeolite bodies prepared via procedure I resembles the spectrum of the ZSM-5 nanoparticles (Figure 8a,b). The absence of a resolved peak at 490 cm^{-1}, which is the most intense "amorphous" Raman signal, reveals no existence of nanosized nonperiodic domains with atomic arrangements typical of the initial silica glass. However, in the spectrum of the zeolite body obtained according to procedure II, there is still a weak and broad band near

(30) Woolery, G. L.; Alemany, L. B.; Dessau, R. M.; Chester, A. W. *Zeolites* **1986**, *6*, 1.
(31) Ravishankar, R.; Kirschhock, C.; Schoeman, B. J.; Vanoppen, P.; Grobet, P. J.; Storck, S.; Maier, W. F.; Martens, J. A.; De Schryver, F. C.; Jacobs, P. A. *J. Phys. Chem. B* **1998**, *102*, 2633.

960 cm^{-1}, indicating disruption in the T−O network connectivity. Besides, a weak extra Raman scattering between 400 and 490 cm^{-1} is clearly seen, thus revealing faults in the periodicity of the T−O network. Therefore, the degree of structural ordering is higher for samples prepared via procedure I versus procedure II. Thus, for the sample prepared via procedure I, the extra nontwisted TPA deduced from the spectra of as-synthesized samples are placed in the intergrain space, while for the sample prepared according to procedure II, the extra nontwisted TPA are trapped in large-size defects and voids inside structural domains of poor crystallinity.

Discussion

All three synthesis approaches proposed in this study transform successfully the amorphous silica grains into ZSM-5 bodies built of relatively uniform zeolite nanocrystals. Combined analysis of the obtained materials shows that the ZSM-5 bodies synthesized according to procedures I and III have higher crystallinity and larger crystals with respect to the material synthesized according to procedure II. Although the preparation procedures I and III differ substantially, the structural features of the ZSM-5 bodies are fairly similar, which suggests that the application of seeds in the latter does not play an important role in the transformation of the amorphous silica grains.

The aged initial solution used for inducing zeolite crystallization in procedure II contains preorganized units[27,28] of several nanometers. At least a part of these entities is comparable in size to the mesopores of the amorphous silica grains. The penetration of these preorganized units in the volume of silica grains seems to promote a very uniform nucleation process and, as a consequence, the formations of much smaller ZSM-5 nanocrystallites with respect to procedures I and III. It is worth recalling that the synthesis solution used in this procedure did not contain silica; that is, the alumina and SDA should migrate readily in the grains' bulk and react with the silica. This synthesis approach seems to be the most promising, because it provided extremely closely packed and uniform ZSM-5 nanoparticles, which built zeolite bodies containing mesopores with a relatively narrow distribution. Moreover, procedure II led to a higher silica conversion, and the ultimate product had a Si/Al ratio very close to that in the initial overall composition (Si/Al = 47). This sample showed a lower aluminum content, which correlated with the low amount of TPA determined by TG analysis (TPA $\approx$ 10.4 wt %).

Although no special tests of the mechanical properties of ZSM-5 bodies obtained according to the described preparation procedures were performed, the differences can be easily distinguished. Neither as-synthesized nor calcined ZSM-5 bodies show tendency to disintegrate into smaller pieces with time, and therefore different laboratory operations can be performed without risk of breaking the particles. The closely packed zeolite nanocrystals obtained according to procedure II needed the most effort to be grinded in a mortar.

Conclusions

Closely packed ZSM-5 nanocrystalline bodies were obtained by hydrothermal transformation of porous silica grains with a size of about 60 μm. Zeolitized grains retain the morphological features and size of the initial amorphous silica grains. Thus, self-bonded all-zeolite bodies that could find different applications were obtained.

Three different synthesis approaches were employed for the synthesis of closely packed ZSM-5 zeolite bodies: (I) direct hydrothermal treatment of the amorphous silica grains with a ZSM-5 precursor solution; (II) seeding of the silica grains with 2−10 nm preorganized ZSM-5-type units followed by a hydrothermal treatment with a silica-free synthesis solution; and (III) seeding of the silica grains with 50 nm ZSM-5 crystals followed by hydrothermal treatment with a ZSM-5 initial precursor solution. Depending on the synthesis procedure, nanozeolite ZSM-5 bodies with high X-ray crystallinity and different particle size, levels of packing, and mechanical properties were synthesized. The average size of the zeolite nanocrystals decreases in the following order: I $\geq$ III > II, while the mechanical properties decrease in the opposite direction. Thus, procedure II provided very small ZSM-5 crystallites (about 40 nm) building zeolite bodies with good mechanical properties and textural mesopores with a relatively narrow pore size distribution.

Acknowledgment. The financial support of the DFG-CNRS bilateral program and BFHZ is greatly acknowledged.

CM030640B